On the Dielectric Breakdown of Water: An Electrochemical Approach

Marek Szklarczyk, Ramesh C. Kainthla, and John O'M. Bockris*

Surface Electrochemistry Laboratory, Department of Chemistry, Texas A&M University, College Station, Texas 77843-3255

ABSTRACT

The dielectric breakdown of water under static fields has been studied by current-potential relation for six metals. The relations are quasi-linear up to a current density of a few A-cm^{-2}. The limiting current continues for a few volts to a few hundred volts, depending on the metal. A glow develops at the electrode and becomes continuous at the end of the plateau, where the current density increases irregularly (breakdown). The breakdown potential does not depend on the field in the water. It occurs at about the same current density for most of the metals. When electrolytes are added, the cell potential at the breakdown is decreased. Adsorbed layers and organic coatings increase the breakdown potential. Electrical energy storage in water is increased by ~10 times by coatings. The breakdown potential decreases with increase of log of rate constant for hydrogen evolution on the various electrodes and with the corresponding work function. The cell potentials for breakdown correspond to fields in the dielectric below that needed to dissociate it. The limiting current is caused by the formation of a H_2-steam layer at the interface, which causes increase in the electrode potential at constant current. The H_2-steam layer plasmolyzes. When the Fermi level in the cathode reaches the conduction band of water, electrons enter the water and remain stable therein. They interact nonadiabatically with water and are the head of streamers. An analogous model holds for holes in the valence band. "Dielectric breakdown" depends on the Fermi level of the electrons in the condenser plate and the semiconductor characteristics of water. It can be eliminated by modifying the electrode surface.

It is well known that when an increasing electric field is applied to the dielectric between two condenser plates, a value of electrical potential between the plates is reached at which "breakdown of the dielectric" occurs. In solids, this event is irreversible. Dendrite-like "spikes" strike out between the plates, and the material of the dielectric undergoes chemical or electrochemical decomposition. In gases and liquids, the breakdown is temporary, and the dielectric recovers when the field is removed.

In recent times, interest in creating particularly high electric fields in pulse power technology has re-evoked interest in the mechanism of dielectric breakdown, particularly with respect to water, which is the preferred dielectric in large scale applications.

The mechanism of breakdown in liquids is not well understood. Several stages occur. So called "streamers" develop between the electrodes (1). The latter phenomenon proves that some degree of decomposition of the water dielectric between the condenser plates occurs.

However, the charges which constitute the streamer head emanate from the surface of the condenser plates, *i.e.*, the electrodes, and for this reason, interfacial charge transfer may be an important, and perhaps the rate-determining step in breakdown.

The techniques used for the study of dielectrics (1-15) have involved the application of voltage pulses to systems of different geometries with electrode separations in the range of 0.2-2.5 cm. Among the liquids studied have been pure water and a number of organics. Optical and electrooptical approaches have been used (14, 15).

In this paper, a study of the current-potential relation under steady-state conditions has been made up to and past the potential at which light emission at the electrode begins. The steady-state condition, rather than transient pulses, was studied because it is more demanding, *i.e.*, breakdown occurs at lower applied voltages, than it does under pulses regimes.

Experimental

Figure 1 shows the schematic diagram of the experimental setup used. The experiments were carried out sometimes in a glass, but mainly in a Teflon, cell.

Water purification methods.—The methods used to purify water were (*i*) four-fold distillation, the third distillation being over KMnO$_4$, (*ii*) double distillation followed by passage through an ion exchange column, and (*iii*) once-distilled water passed through "Millipore-Q sys-

tem" which consists of four cartridges, two of which are ion exchange while the other two are used to remove organic impurities from water before passage through a 0.1 µm filter.

The highest resistivity of water (16-18 MΩ-cm) and lowest concentration of organics (<40 ppb) was obtained using the third method (*i.e.*, Millipore Q system). The concentration of the organic impurities was determined by oxidizing them with persulfate (K$_2$S$_2$O$_8$) to CO$_2$ and measuring the amount of CO$_2$ with total organic carbon infrared analyzer (Model 700).

The purified water was then transported to a pre-electrolyzer (Fig. 1). The pre-electrolysis cell had two large area platinum electrodes. Impurities were removed by adsorption on to the electrodes and/or by oxidation. The electrolysis cell voltage was 30-40V and the time ~24h. The water in the pre-electrolysis cell was bubbled with high purity argon. The Ar itself was purified by passing it through a copper column maintained at 260°C and another column containing molecular sieves (4A, 13 ×).

Finally, the water was transported under argon pressure to the experimental cell.

Preparation of electrodes.—The working electrode was a microelectrode with planar tip and the counterelectrode was a 0.6 cm diam plane platinum electrode. The elec-
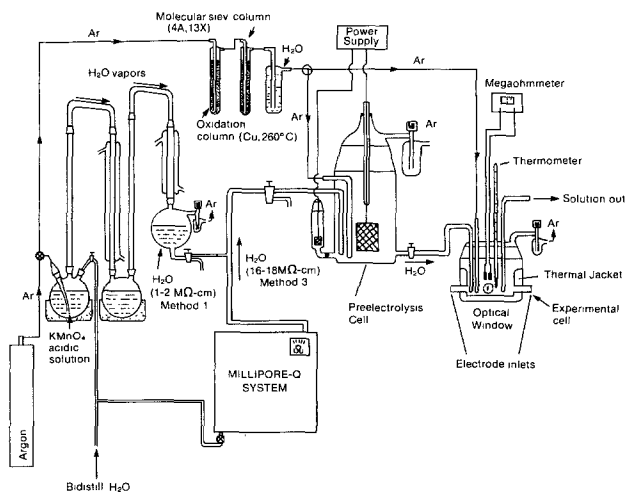

Fig. 1. Schematic diagram of experimental setup

trodes consisted of Pt, Cu, Fe, Ni, Au, and Co. The diameters of the electrodes were; Pt, 10, 25, and 100 μm; Cu, 127 μm; Fe, 102 μm; Ni, 23 μm; Au, 76 μm, and Co, 76 μm. The purity of the metals was >99.9%.

The electrodes were sealed into a soft glass tube. Before each experiment the surface was mechanically polished with alumina paste. The electrode surface was monitored with an Olympus optical microscope (200 times magnification).

Before the breakdown experiments each electrode was activated by cathodic-anodic polarization.

The distance between the working and counterelectrode was measured by means of a digital micrometer. It was adjusted over a range of 2-10 mm. After preparation, the electrodes were mounted in the cell which was then filled with the pure water, as described above. Temperature and resistivity probes were introduced into the cell and monitored the state of the solution.

Most measurements were carried out in the Teflon cell, which had provisions for illumination of the interior using a light pipe. The cell was fitted with a quartz window to observe luminescent phenomena associated with breakdown. The electrode was polarized cathodically.

Electronic equipment.—Electrochemical treatment and characterization of the electrodes were carried out using a potentiostat fitted with sweep generator (Pine Instruments Company, Model RDE 4). The X-Y recorder was from Yokogawa, Model 3023.

For studies of electrical breakdown phenomenon, a high voltage dc power supply (Hipotronics, Model 830C), electrometer (Keithley, Model 616), multimeter (Hewlett Packard, Model 3466A), and X-t recorder (Fischer, Model 5117) were used.

The conductivity of water was measured using a conductance meter (Cole Parmer, Model 1481-60) and water purity meter (Barnstead, Model PM-5D).

Results

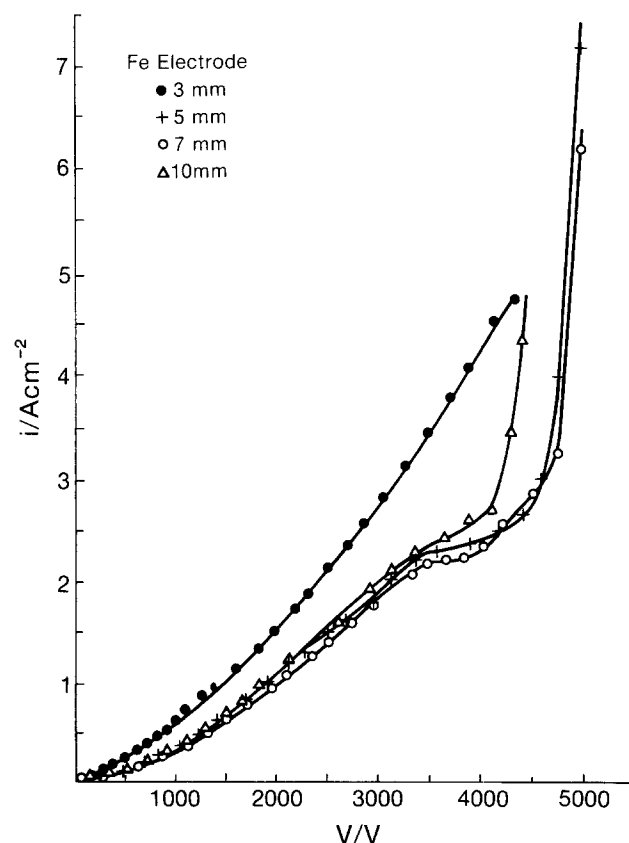*The study of current-voltage behavior.*—Figure 2 shows the dependence of current density for hydrogen evolution on the cell potential for an Fe electrode with different separation between the electrodes. In the low voltage region (first few hundred volts), the current varied exponentially rather than linearly with the potential. In the higher potential region, above about 4000V, a sudden increase in the current density occurred. An intermediate region (3000-4000V) was observed, in which the current density forms a plateau. A glow discharge around the electrode was observed near the end of the plateau. The current density at the start of flashes was around ~2.5 A-cm^{-2} and was independent of the distance between the electrodes. In the region after the beginning of the plateau, the glow was periodic, reoccurring at intervals of about 30-50s. At higher currents, the glow became continuous. The linear extent of the glow was of the order of 1 mm.

Figures 3 and 4 show the current-density as a function of cell-voltage for electrodes of various metals. The I-V curves have the same characteristics although the plateau was well resolved only for Pt, Fe, and Au.

The I-V characteristics for Pt, Au, Cu, Ni, and Co, when measured as a function of distance between the electrodes, had the same features as in Fig. 2. The measurements showed that the breakdown occurred at a certain current density but was not dependent on the electric field in the bulk of solution.

The influence of electrolytes on the breakdown potential.—To study the influence of electrolytes on the breakdown potential, sodium chloride and ammonium hydroxide were chosen. The concentrations were in the range from 3×10^{-6} to $5 \times 10^{-4}M$ and from 1×10^{-4} to $5 \times 10^{-3}M$, respectively. The corresponding I-V curves are plotted in Fig. 5 and in Fig. 6. The breakdown potential decreased with increase in concentration of conductance (Fig. 7 and 8).

Effect of surface modification.—The influences of sulfide layer (16, 17), paraffin film, and a black wax layer were studied.

Sulfur was deposited by means of electrochemical adsorption on the surfaces. After polishing, the electrodes were placed in an electrochemical cell containing 1M H_2SO_4 solution for the activation of their surfaces by means of the potentiodynamic sweep method. After this
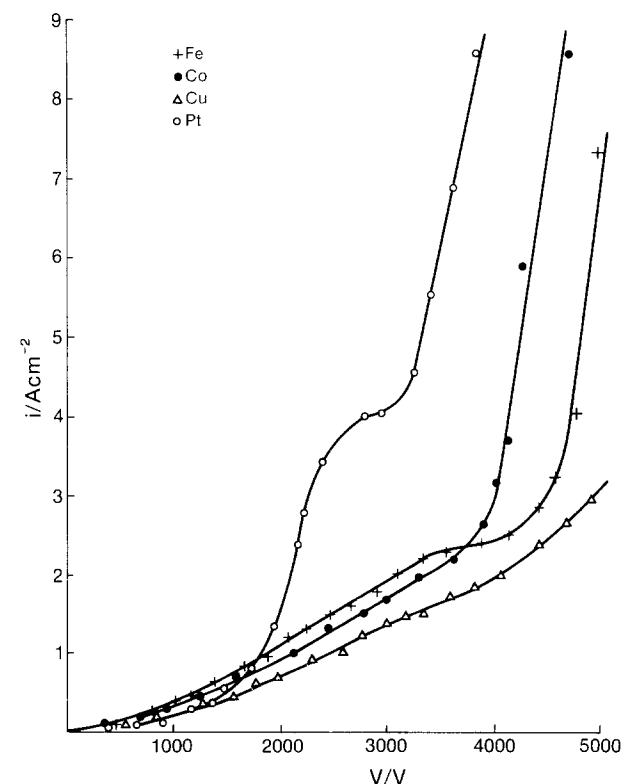
Fig. 2. The *i-V* dependence for Fe electrode for different spacing between the cathode and the anode.

Fig. 3. The *i-V* dependence for different cathode materials for the same spacing between the cathode and the anode.
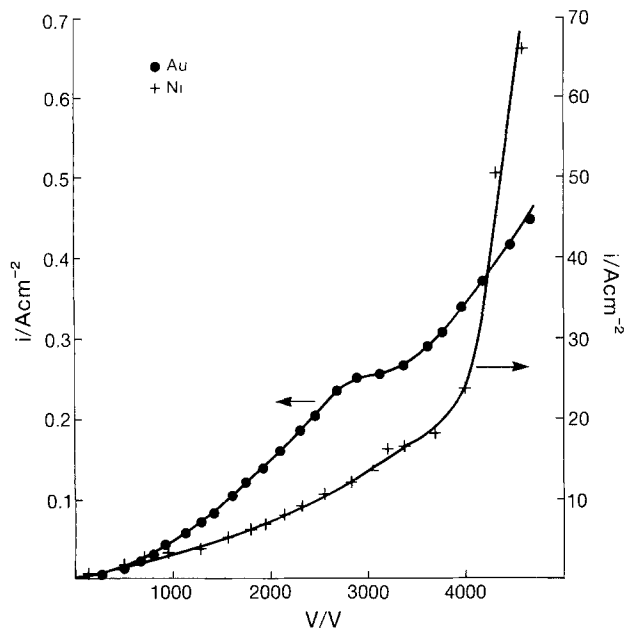
Fig. 4. The *i-V* dependence for Au and Ni electrodes for the same spacing between the cathode and the anode.

step, one of the electrodes was placed in a cell containing $0.1M$ Na_2S + $1M$ Na_2SO_4 solution. The adsorption of sulfur was carried for 40 min. It was monitored by registration of current-potential dependencies and shifted the H_2 evolution reaction by ~400 mV in the cathodic direction.

The poisoning of the electrode increased the breakdown voltage by ~2000V in the case of Pt electrode (Fig. 9).

In Fig. 10, curve a was obtained for a paraffin film thickness about four times smaller than that for curve b. A remarkable increase in breakdown potential by 3-4 kV in comparison with that at a bare Pt electrode was observed.

The influence of a film of black wax on the breakdown potential is shown in Fig. 11. The shift varies from 6 to 25 kV depending on the thickness of the film. With 0.5 mm thick film, the breakdown potential was >30 kV.

Discussion

The main results to be interpreted are:

1. The form of the I-V curve.—A schematic is in Fig. 12. The section below about 2-3 $A\cdot cm^{-2}$ is that expected in terms of the electrode kinetics for H_2 and O_2 evolution in a solution of very low conductance. Then follows a plateau region, extensive for some electrodes, hardly distinguish-
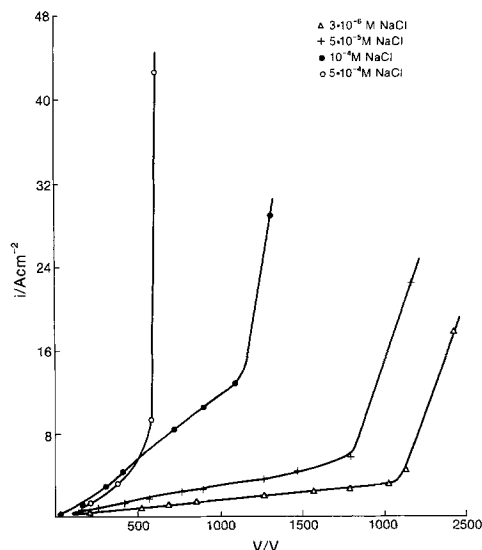

Fig. 5. The *i-V* dependence for Pt electrodes in different concentrations of NaCl in high purity water.
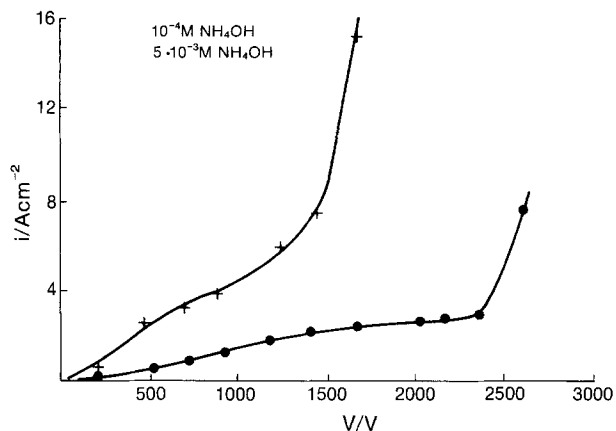

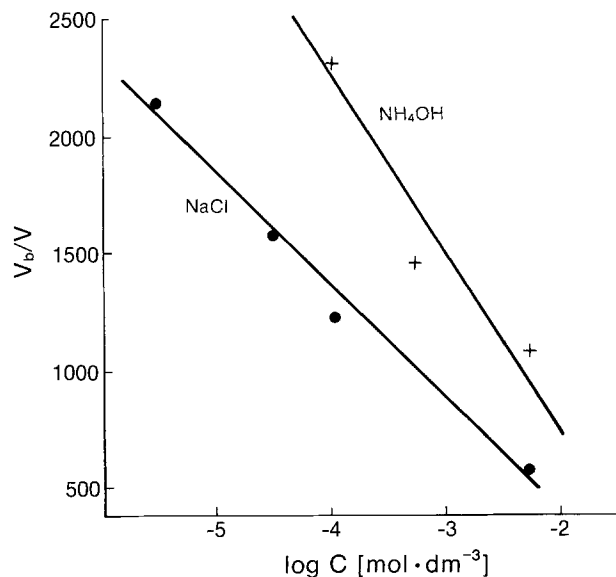Fig. 6. The *i-V* dependence for Pt electrodes in different concentrations of NH_4OH in high purity water.

Fig. 7. The dependence of the breakdown potential (V_b) on the log of concentration (log C) of NaCl (●) and of NH_4OH (+).

able for others, though always present. At the high potential end of the plateau a glow is observed, at first sporadically but continuously at higher potentials. The current increases sharply and becomes irregular.

2. Dependence of the breakdown on cell potential.—The breakdown is not dependent on the field strength in the bulk. It begins when the current density has reached a value of a few $A\cdot cm^{-2}$.

3. Electrode glow.—The glow is blue-white in color.

4. Electrode materials.—The breakdown voltage decreases linearly with increase of log i_o for the hydrogen evolution reaction of the cathode material and with work function.

5. Effect of electrolyte added to pure water.—The breakdown potential is lowered with the increase of conductance, *i.e.*, breakdown is not primarily dependent on the cell potential.

6. Adsorption.—Adsorption on the electrode of materials which inhibit the hydrogen evolution reaction, increases the breakdown potential. A 0.5 mm coating of the electrode with black wax increases the breakdown potential to >30,000V.

Electrode kinetics before breakdown.—The cell voltage for an electrochemical cell can be calculated from

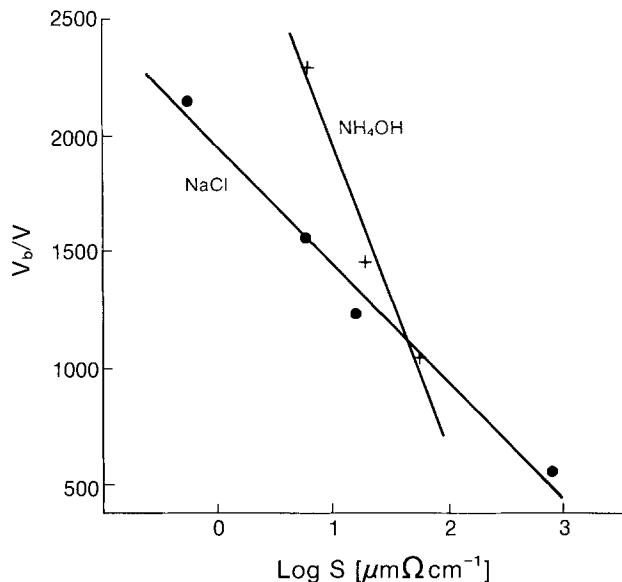$$E_{cell} = E_{rev} + \eta_{a,c} + \eta_a - \eta_{c,c} - \eta_c + IR$$

Fig. 8. The dependence of the breakdown potential (V_b) on the log of conductivity (log S) of NaCl (●) and of NH_4OH (+) solutions.
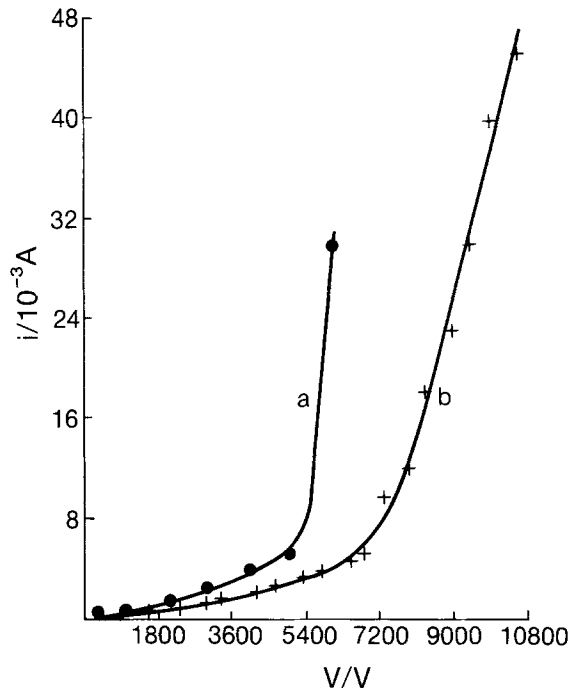

Fig. 10. The *i-V* dependencies for Pt electrode covered with (a) 0.1 and (b) 0.4 mm thick film of paraffin.

and for the anodic reaction on Pt

$$i_{o,a} = 10^{-10} \cdot (a_{H^+})^{0.5} \cdot (p_{O_2})^{0.125} \qquad [5]$$

For pure water, where $a_H = 10^{-7}$

$$i_{o,c} = 10^{-6.5} \cdot (p_{H_2})^{0.25} \qquad [6]$$

and

$$i_{o,a} = 10^{-13.5} \cdot (p_{O_2})^{0.125} \qquad [7]$$

The overpotential due to concentration polarization is

$$\eta_{c,c} = (RT/2F) \ln [1 - \{i/i_L\}] \qquad [8]$$

where i_L is the diffusion limited current, given by

$$i_L = (Dn\mathbf{F}c°)/\delta$$

The solution resistance $R = \rho l/A$, where A is the electrode area, l is the separation between the electrodes, and ρ is the solution resistivity. Thus

$$IR = i\rho l \qquad [9]$$

The above equations were used to calculate the *I-V* curves. For current densities varying from 10^{-13} to 10^{-9}
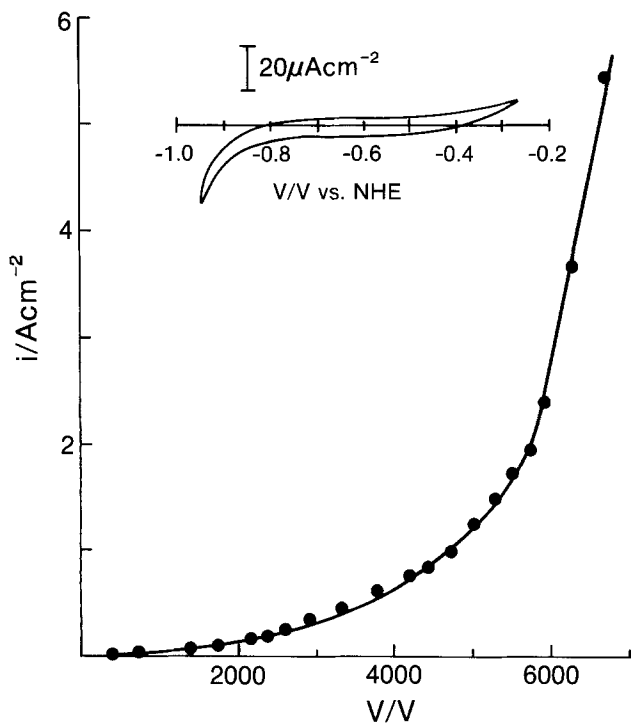

Fig. 9. The effect of poisoning the electrode surface with sulfide on the *i-V* characteristic of the Pt electrode in pure water. Inset, potentiodynamic curve for the poisoned electrode in H_2SO_4 solution, showing the shift in the H_2 evolution potential.

where E_{rev} for an electrochemical cell where the cathodic and anodic reactions are H_2 and O_2 evolutions, respectively, is given as

$$E_{rev} = 1.23 + (RT/2F) [\ln(p_{H_2}) + \ln(p_{O_2})^{0.5}] \qquad [1]$$

The overpotentials (η's) calculated using the Butler-Volmer equation (28) gives ($\alpha = 0.5$)

$$\eta_a = (2RT/F) \sinh^{-1} (i/2i_{o,a}) \qquad [2]$$

and

$$\eta_c = -(2RT/F) \sinh^{-1} (i/2i_{o,c}) \qquad [3]$$

For the cathodic reaction of hydrogen evolution on Pt

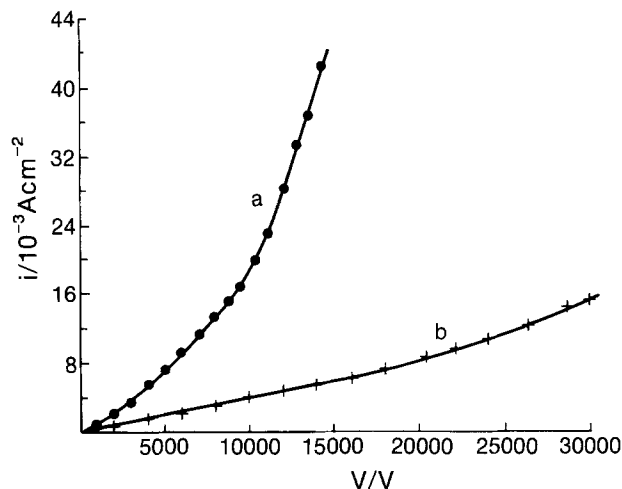$$i_{o,c} = 10^{-3} \cdot (a_H)^{0.5} \cdot (p_{H_2})^{0.25} \qquad [4]$$

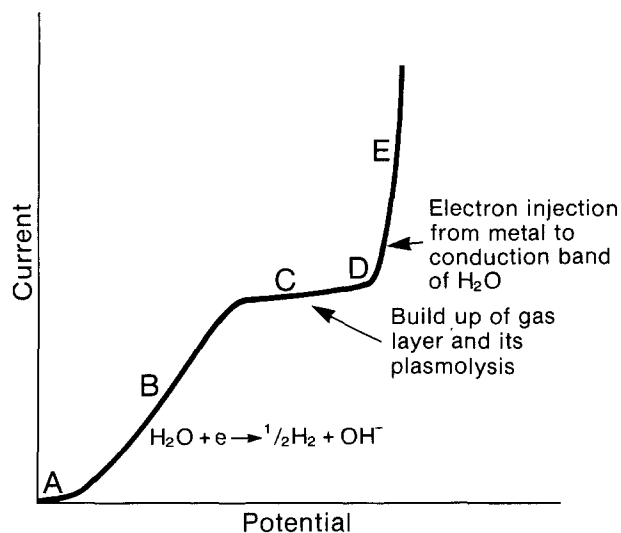Fig. 11. The *i-V* dependencies for Pt electrode covered with (a) 0.1 and (b) 0.5 mm thick film of black wax.

Fig. 12. Schematic representation of the *i-V* curves obtained with different electrodes in pure water.

A-cm^{-2}, the cell voltage is proportional to log i and the line has a slope of 120 mV/decade. Because of the low concentration of a_{H^+}, the limiting current density is 2×10^{-9} A-cm^{-2}. Higher current densities can be obtained, only if H$_2$O is assumed to be the source of carriers. In this case log i-V has a slope of 120 mV/decade for current densities up to 10^{-6} A-cm^{-2}. For current densities $>10^{-6}$ A-cm^{-2} the current is limited mainly by the solution resistance. In the lower current density range, p_{O_2} and p_{H_2} have an effect, but this becomes negligible above 10^{-6} A-cm^{-2}.

The equations derived above were used to fit the experimental curves. Figure 13 shows the experimental *I-V* points and the calculated points. The experimental and calculated curves match well for cell voltages up to 120V. Thus, in this low cell voltages the experimental curves follow the modified Butler-Volmer equation.

Calculation of electric field for the dissociation of water in the bulk.—The electric field necessary for possible dissociation of water caused by the effect of the field between the electrode on the dipoles is given by $E_D = \Delta H/\mu$, where μ is dipole moment of water molecule. With $\Delta H = 286$ kJ-mole^{-1} (18) and $\mu = 2$ Debye, $E_D = 7 \times 10^8$ V-cm^{-1}, which is higher than the electric field strength in the solution.

Similarly, the field needed to ionize water is given by $E_I = I/\mu$ where I, the ionization energy of water is equal to 12.6 eV. Use of appropriate values gives, $E_I = 3 \times 10^9$ V-cm^{-1} which is decisively higher than the field in the solution.

In the usual breakdown experiments the applied electric field is in the order 10^5-10^6 V-cm^{-1}, while in the electro-

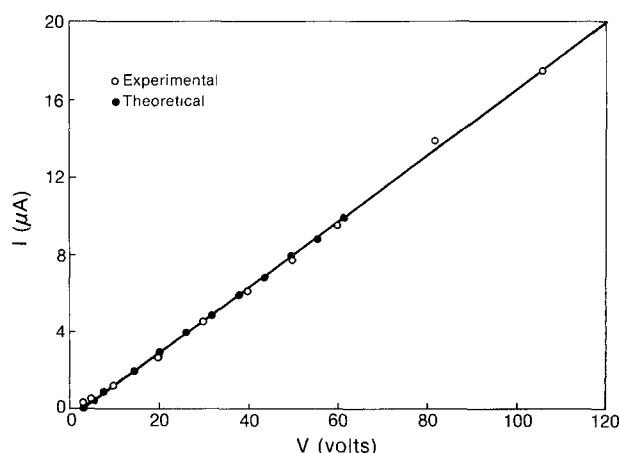chemical double layer the field is of the order 10^7-10^8 V-cm^{-1} (18).

Calculation of the field between the electrodes.—In most of the calculations it is assumed that the field between the electrode is constant and given by the cell voltage divided by the distance between the electrodes. This is true if the electrodes are of infinite dimensions (or the distance between electrodes is smaller than the diameter of the electrodes). If the distance between the electrodes is more than the diameter of the electrode, as in most studies of the dielectric breakdown, the electric field will depend on the dimension and geometry of the electrodes and the location of the point with respect to the electrodes. The potential at a point in the liquid due to charge on two parallel plates (electrodes) can be calculated (19) by taking small areas on the electrode, writing an equation for the voltage at these points and summing over the whole areas of the plates.

Consider the plates to be in the *x,z* planes, located at $y = 0$ and at $y = y_2$ with charge densities of σ_1 and σ_2, respectively. The point P where voltage and electric field is to be calculated has coordinates of (x_1,y_1,z_1). In an infinitesimal area da located at $(x,0,z)$ in the lower plate there is an electric charge $\sigma_1 da = \sigma_1 \, dxdz$, and directly above it in the upper plate at a point (x,y_2,z), there is electric charge $\sigma_2 \, da = \sigma_2 \, dxdz$. The distance from the electric charge in the lower plate to the point P is

$$r_1 = [(x-x_1)^2 + y_1^2 + (z-z_1)^2]^{1/2}$$

and from the electric charge in the upper plate to point P is

$$r_2 = [(x-x_1)^2 + (y_2-y_1)^2 + (z-z_1)]^{1/2}$$

Thus the voltage at point P is given by

$$V = (1/4 \, \pi\epsilon) \int (\sigma da/r)$$

$$= (1/4 \, \pi\epsilon) \int\int [(\sigma_1/r_1) + (\sigma_2/r_2)] \, dxdz$$

where the integration is to be carried out over the dimensions of the plates.

The integration can be solved in the closed form if the plates are assumed to have infinite dimensions. In a practical situation where the dimensions are finite, the integral cannot be solved in the closed form. Consequently, the integration has to be carried out numerically.

As the electrodes in our studies have a circular face, the equations given above were transferred into cylindrical coordinates. Two plates with radii of a_1 and a_2, separated by a distance b were considered. The first plate is assumed to be at $z = 0$ and has a charge q_1 while the second plate is at $z = b$ and has a charge q_2. Because of the circular symmetry, potential V and electric field E are dependent only on r and z.

Figure 14 shows the electric field distribution as a function of distance from the working electrode, for a system with a microelectrode of 100 μm diameter and a counterelectrode of 0.6 cm diam with a distance of 0.3 cm between

Fig. 13. The comparison of experimental data with theoretical points calculated using modified Butler-Volmer equation.
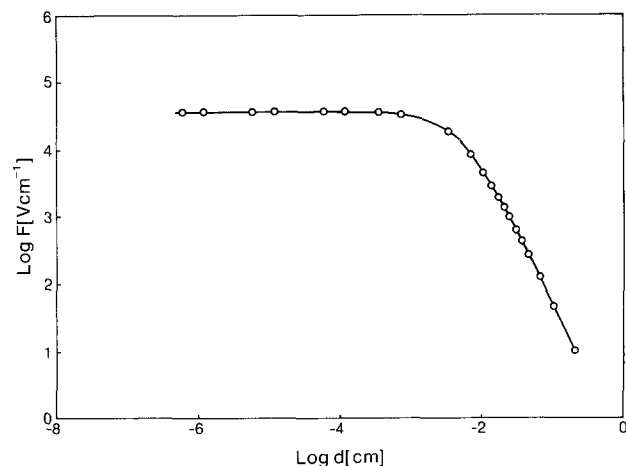

Fig. 14. The log-log dependence of electric field on distance from the working electrode.

them. The total charge on each electrode has the same magnitude but different sign.

The figure shows that the field near the electrode is higher than the field in the solution or near the counter-electrode. The figure also shows that for distances smaller than the radius of the smaller electrode, the field is almost independent of the distance from the electrode.[1] The maximum value of field near the smaller electrode is ~4 × 10⁴ V-cm⁻¹ which is much smaller than the field required in the bulk to dissociate water.

Hence, the breakdown of water is not due to field in the bulk of the water, but to happenings at the metal-water interface.

The i-V relationships up to breakdown.—The *i-V* relations (Fig. 12) can be subdivided into those with a limiting plateau region of several hundred volts (Fig. 2-4 for Fe, Pt and Au), and those (Fig. 3 and 4 for Co, Cu, and Ni) in which the plateau region is a mere inflection.

In Fig. 15, the *I-V* curve of Fe is plotted together with the *dV/dI* values. In the initial region up to the plateau, the situation is that of the electrolysis of water. The *I-V* relation is dominated by the resistance of the solution.

The change of species from which H_2 is evolved from H_3O^+ to H_2O has been studied by Bockris *et al.* (20) in the *pH* range between 2 and 5. As the source of the protons for a current density above *ca.* 10^{-8} A-cm⁻² is water, the plateau region cannot be seen as the (activationless) limiting current of electron transfer as discussed by Despic and Bockris (21) and particularly by Krishtalik (22).

The current is constant in the plateau region and does not fall because steam is evolved sporadically and will allow a continued, but restricted, evolution of hydrogen within this region.

The plateau region.—The length of the plateau can be as much as 800V, but some 99% of this would be in the solution as the ohmic drop. Thus, the likely change of electrode potential corresponding to the several hundred volts drop in the solution would be of the order of 1V.

Thus, when the potential reaches the level C, at the beginning of the plateau, two processes may combine to prevent further increase of current density.

---

[1] Such behavior is consistent with that expected from simple electrostatics; according to which the field sufficiently near to a charged plate is $4\pi\sigma/\epsilon$, *i.e.*, independent of distance.
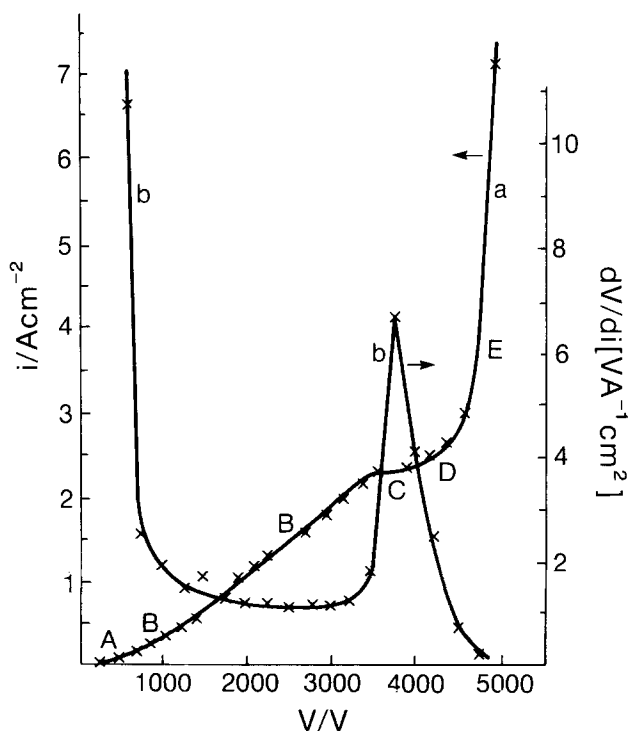

Fig. 15. The (a) *i-V* and (b) *dV/di* dependencies for Fe electrode in pure water.

1. At the current-density of a few A-cm⁻² so much H_2 will be evolved that access of the water to the electrode becomes increasingly difficult. At the same time, local heating will give water vapor formation further obscuring contact between solution and metal.

2. Another cause of a limiting current will correspond to the nontransport controlled limiting current density mentioned above. Thus, in the region of electrode kinetic control, electrons tunnel to the vibrational levels in the water molecules which can be exceeded for sufficiently negative values of the electrode potential.

In the plateau region, an intermittent occurrence of a glow is seen. An interpretation of this may be in terms of electron levels in the metal which by now have become sufficiently high to start a plasmolysis of the hydrogen-steam layer. It is known that, for example H_2, O_2, O_3, HO_2, H_2O_2, and $OH°$ are formed in the plasma (23). The intermittency of the glow at this stage may arise from a buildup of the concentration of ions, radicals, and electrons, followed by their recombination (which would give rise to the radiation which constitutes the glow), then rebuild up, etc.

Under these conditions, the electron levels in the electrode can be represented as shown in Fig. 16.

Breakdown.—The position of the Fermi level of electrons in the electrode at the end of the plateau, where a large increase in current occurs, may be estimated as follows (in the case of Fe electrode for which different regions in the *I-V* characteristics are clearly differentiable):

At zero cell potential the Fermi level is at −4.1 eV. Taking i_o for Fe in pH 7.0 solution as $10^{-9.1}$ A-cm⁻², at the beginning of the plateau, where the current density is ~4.5 A-cm⁻², the overpotential will be

$$\eta = -120 \log (4.5/10^{-9.1}) = -1.17V$$

Therefore, the Fermi level at the beginning of the plateau will be at −4.1 + 1.2 = −2.9 eV.

Now the length of the plateau region is ~800V which may be related to the electrode potential and hence Fermi level change as follows:

In the region from A to C (for Fe), a change in cell potential of ~3500V results in change of Fermi level of ~1.17 eV. Thus, an 800V change would be equivalent to ~0.27 eV change in the Fermi level. However, in the plateau region no further increase in the rate of electron transfer to the solution occurs, so that an increase of total cell potential is likely to increase the electrode potential (and hence the Fermi level) by a greater degree (per unit of cell potential change) than that at earlier conditions when an increase of charge on the electrode surface resulted in an increase of the rate of loss of electrons across the interface.

Taking now the ratio of *dV/dI* (Fig. 16) for region CD to region BC, it seems acceptable to assume an enhanced rate of increase in the Fermi level change, as a function of the cell potential in the plateau region of about six from that calculated from the condition in the region AC. Hence, the expected change of E_F over the plateau region would be about 1.6 eV and the value of the Fermi level, therefore, about − 1.3 eV (−2.9 + 1.6).

Pure water can be regarded as a semiconductor (24). The corresponding diagram is shown in Fig. 17 which shows that the position of the conduction band of water is between 0 and −1.2 eV.

From the above estimates, at the end of the plateau region the position of the Fermi level of electrons in the metal is ~−1.3 eV. Thus, it is hypothesized here that the breakdown occurs (point D in the Fig. 15) when the Fermi level of electrons in the cathode becomes equal to the conduction band of water.

Under these conditions, the situation is as depicted in Fig. 18.

One of the more outstanding facts about the prebreakdown region is that the breakdown occurs at approximately the same current density. (That is for 11 out of 14 systems this current density is 5 ± 2 A-cm⁻². Three further systems extend this limiting current from 0.3 to 25 A-cm⁻²).

An interpretation of this can be given in terms of the rate at which electrons need to be injected into the hydrogen-steam layer at the interface in order to make it into a
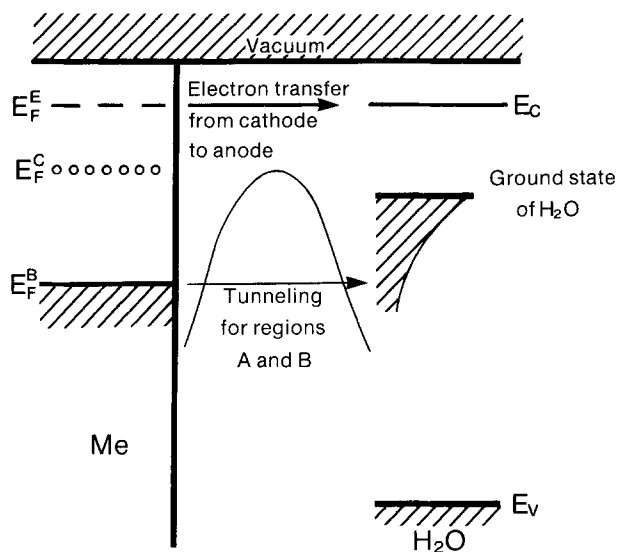
Fig. 16. The schematic representation of the Fermi level of the electrons in the electrode and different levels in H_2O. E_F^B, E_F^C and E_F^E correspond to the position of the Fermi level corresponding to the regions B, C, and E, respectively, of the *i-V* curve. E_V and E_C represent the valence and conduction bands of water. Barrier for the electrons at the metal-solution interface is also shown.

plasma.

As noted, the plasma begins sporadically, corresponding to a charge-up and discharge. But to maintain itself, it needs a minimum number of electrons per unit area in time, and this is equivalent to about 5 A-cm^{-2}.

Correspondingly, it is clear that the length of the plateau varies rather considerably with varying metals, from a maximum of 800V for iron, down to a mere inflection for copper and nickel.

Qualitatively, this change can be rationalized in the sense that the plateau begins when the gas layer precludes further increase of current density, but the potential at this point will be variable, depending upon the Fermi level of the metal and the overpotential needed to reach the constant current density at which the plasma forms.

In order, therefore, to reach the conductance band of water (a constant independent of metal), different increases of potential will be needed for each metal, *i.e.*, a length of the plateau will be a metal-dependent parameter.
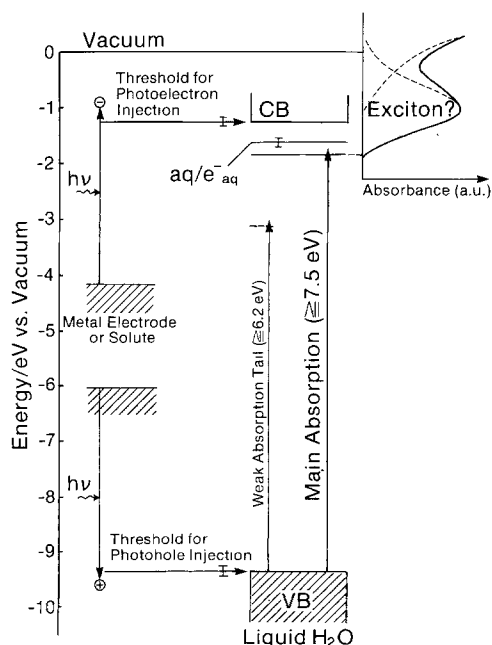

Fig. 17. Schematic representation of water as semiconductor [after Watanabe and Gerischer (24)].
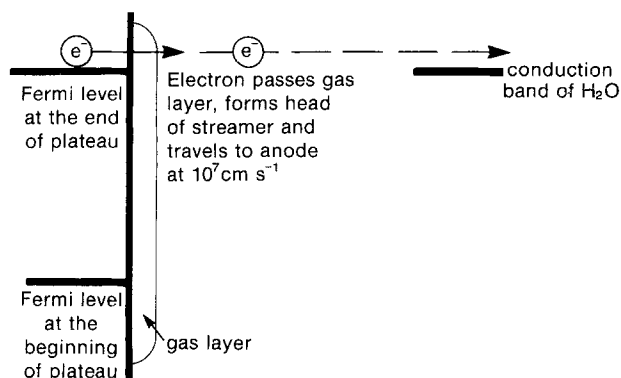

Fig. 18. Schematic representation of the transfer of electrons from metal to the conduction band of water in the region at D and after the breakdown (region E).

Streamers.—In water, dielectric breakdown is associated with the phenomenon of streamers (6, 13). These appear to be luminous lines which pass sporadically between cathode and anode and are a major characteristic of the breakdown process in water. The velocity of these streamers has been measured to be as high as 10^7 cm-s^{-1} (0.1% of the velocity of light) (6, 13). Such a velocity can only be associated with the flow of electrons.

Now, the ejection of electrons from electrodes into the solution is a well-studied phenomenon. It is to be distinguished from the normal phenomena associated with electrolysis in which electrons tunnel through barriers of a few angstroms at the electrode and create, *e.g.*, hydrogen atoms in cathodic processes, *i.e.*, do not form the solvated electronic states. Electron ejection normally involves solvated electron formation (25). It was first studied by Hart and Boag (26). However, it is well known that the ejection of electrons into aqueous solutions cannot occur normally in thermal electrolytic processes because the potential generated there is too low (*i.e.*, insufficiently positive) on the absolute scale. On the other hand, the ejection of electrons into aqueous solutions can be studied photoelectrochemically (27). Correspondingly, it is possible to eject electrons into nonaqueous solutions thermally as was shown by Barker and co-workers (28).

The study of the lifetime of hydrated electrons has been carried out by Johnson (29), who found their lifetime to be in the region of 10^{-9} s. Assuming a distance of 1 cm between cathode and anode, it is seen that the electron passage at 10^7 cm-s^{-1} would take about 100 times longer than the lifetime. Thus, hydrated electrons cannot pass between cathode and anode.

If consideration be given to the high velocity of the electrons concerned, one can expect a nonadiabatic interaction to occur in respect to the electrons coming to the water molecules, in contrast to the adiabatic which will tend to occur with the production of H_2 when the electrons are ejected from electrodes photoelectrochemically into ionic solutions (*i.e.*, when solvated electrons with a lifetime of about 10^{-9} s are formed).

Thus, consider a streamer-head velocity of 10^7 cm-s^{-1}. Taking a water molecule as having a diameter of around about 3Å, the time the electron remains in the vicinity of a water molecule is some 3 × 10^{-15} s. However, the vibrational frequency of the proton in water is around 10^{14} s^{-1}. Thus, upon the approach of a high velocity electron, as involved in the streamer process, to a water molecule, the nonadiabatic interaction will allow the electron to pass essentially freely through the water (under the influence of a field in the bulk of solution of about 5000 V-cm^{-1}).

In this way, the formation of streamers is given some continuity with the prebreakdown theory developed earlier.

Thus, in summary, the breakdown of the dielectric water—and similarly for other liquid dielectrics—occurs when the potential difference caused by the field applied between the electrodes causes a change in the Fermi level in the electrode so that the electron levels reach the level of the conduction band of the liquid. The field between the

cathode and anode then causes the electron velocity to be around 10^7 cm-s^{-1}, equivalent under a field gradient of 5×10^3 V-cm^{-1} to an electron mobility of 5×10^3 cm^2-V^{-1}s^{-1}. Similar mobilities are known for electrons in solid semiconductors (30).

The discussion given here refers to processes at the cathode. However, analogous processes can be supposed to occur at the anode where the effect of potential would be opposite in direction to that for the Fermi level in the cathode, *i.e.*, the Fermi level would be lowered until it is coincident with the valency band and holes can tunnel from the valency band of the solution and transfer themselves to the anode.

The dependence of the breakdown potential upon the exchange current density for hydrogen evolution and the work function of the substrate.—The experimental relationship obtained with six electrode materials is shown in Fig. 19 and 20.

A qualitative interpretation is easy to make: Fig. 19 shows that the breakdown potential is higher when the hydrogen evolution rate is slow (*i.e.*, small i_o). To reach the critical current density for plasma formation the electrode potential must be increasingly negative for the electrode with lower i_o. Such an increasingly negative value of the
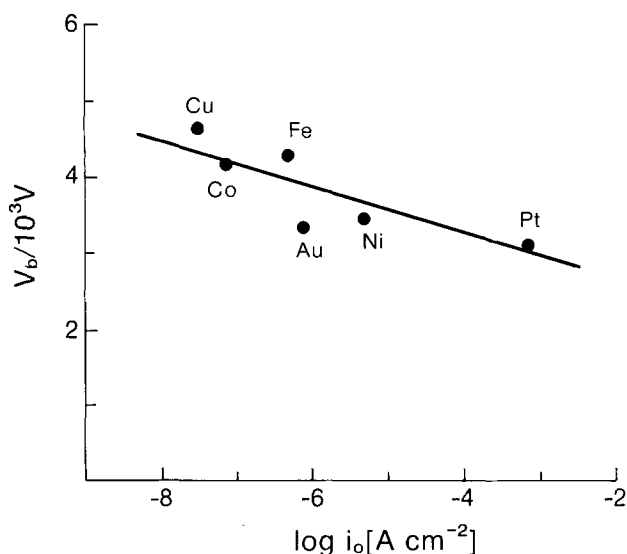

Fig. 19. The dependence of breakdown potential (V_b), on log of exchange current density (log i_o) for hydrogen evolution reaction at different cathodes.
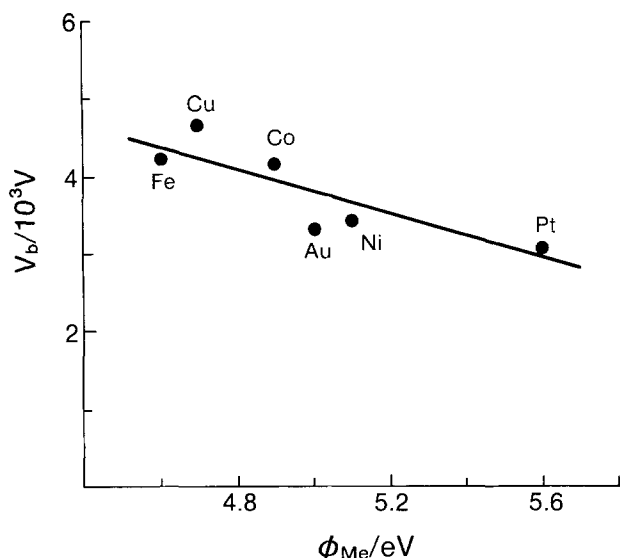

Fig. 20. The dependence of breakdown potential (V_b) on work function (Φ) of the electrode material.

electrode potential would express itself in an increasing cell potential.

The dependence upon work function follows from the dependence found for the hydrogen evolution reaction. It is known (31) that there is an inverse relationship between the exchange current density and the work function such that, with increase of work function, the i_o for the hydrogen evolution reaction gets more. High breakdown values will, therefore, correspond to smaller work functions.

Effect on the breakdown potential of addition of ionic components.—In Fig. 7 is shown the dependence of breakdown potential on the concentrations of sodium chloride and ammonium hydroxide: the breakdown potential may be as small as 500V in the presence of ionic conductors.

This diminution would be consistent with the model, because the field between the two electrodes is not of direct importance. It serves to set up a condition which allows an increase of the potential of the electrode to occur in such a fashion that the Fermi level of the electrons in metal equalizes with the conductivity band of water. If the IR drop is sufficiently small, the total potential difference required for the condition for breakdown will also be smaller than in the case of the lower conductivity (higher IR drop between the electrodes) associated with pure water.

It appears from plots of V_b against log $c_{electrolyte}$ or log $S_{electrolyte}$ (Fig. 7 and 8), that the curves do not extrapolate to the same value of breakdown potential at zero concentration of the salts. There is a suggestion that higher values of the breakdown potential could be obtained, *e.g.*, in the case of ammonium hydroxide, at very low concentrations.

The different slopes of the V_b – log $c_{electrolyte}$ can be qualitatively explained on the basis of different dissociation constant α which causes the number of ions in solution to be different, so that IR and hence V_b values will be different.

Practical aspects: improvement of the breakdown potential in cells involving a water dielectric.—It is desirable to be able to induce higher voltages on condenser plates, with the dielectric being water. The energy storage per unit volume is proportional to the field squared, and therefore the energy stored increases rapidly with increase of voltage.

The adsorption of sulfide on the electrode increases the breakdown potential by about 2000V (Fig. 9). The black wax deposits make the breakdown potential greater (Fig. 11).

The interpretation of this is that in order to reach the conductivity band of the solution, and thus breakdown the dielectric, the electrons must pass through the black wax, and they cannot do this until they reach the conductivity band of wax, which is evidently much higher than that of water.

To es'.mate the energy stored, we note that the system can be represented as shown in Fig. 21.

To calculate the amount of energy stored in the system, it is necessary to find the potential drop in wax and water layers. This can be done either on the basis of Ohm's law using cell voltage, $V = 30,000$V; cell current density, $i = 10^{-2}$ A-cm^{-2}; thickness of wax, $l_{wax} = 0.05$ cm; thickness of water, $l_{water} = 0.5$ cm; water resistivity, $\rho_{water} = 2 \times 10^6$ Ω-cm or Gauss's law.

Calculation based on Ohm's law.—The total resistance R ($=V/I= 30,000/10^{-2}$) is 3×10^6 Ω. As water and wax layers are in series, $R = R_{wax} + R_{water}$. For water, $R_{water} = (\rho_{water} \times l_{water})/S = 2 \times 10^6 \times 0.5/1 = 1 \times 10^6$ Ω.

Therefore, $R_{wax} = 3 \times 10^6 - 1 \times 10^6 = 2 \times 10^6$ Ω, and $\rho_{wax} = (2 \times 10^6 \times 1)/0.05 = 4 \times 10^7$ Ω-cm.

This value is lower than that reported (32). Impurities and water vapor may have been trapped in the layer, causing the drop in the resistivity.

The potential drop in the wax layer is then, $V_{wax} = \rho_{wax} l_{wax} i = 4 \times 10^7 \times 0.05 \times 10^{-2} = 20,000$V.

Hence, the potential drop in water, V_{water} is

$$V_{water} = 10,000\text{V}$$

(The potential drop in the water dielectric for the system with an uncoated Pt electrode was 3000V).
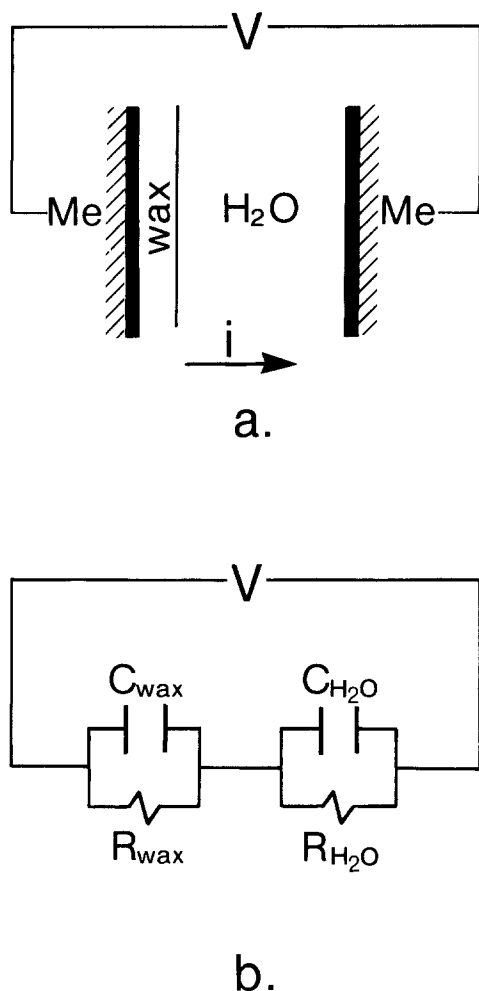
a.

b.

Fig. 21. (a) Schematic representation of water-black wax system and (b) the circuit model of the studied system.

Calculation based on Gauss's law.—As $\int Eds = q/\epsilon_0\epsilon$, where q is free charge, $E_{wax} = q/\epsilon_0\epsilon_{wax}$, $E_{water} = q/\epsilon_0\epsilon_{water}$, and $V_{wax} = ql_{wax}/\epsilon_0\epsilon_{wax}$, $V_{water} = ql_{water}/\epsilon_0\epsilon_{water}$.

Hence, $V_{wax}/V_{water} = l_{wax}\epsilon_{water}/l_{water}\epsilon_{wax} = (0.05 \times 79.0/0.5 \times 2.5) = 3.2$.

As $V_{wax} + V_{water} = 30{,}000V$, $V_{wax} = 20{,}600V$, and $V_{water} = 9{,}400V$.

The ratio of energy stored in water with (E_1) and without wax film (E_2) on the electrode surface is given by

$$E_1/E_2 = (V_1/V_2)^2 = (9400/3100)^2 = 9.2$$

In this calculation, the energy stored in the wax layer has not been included.

Conclusions

1. The breakdown potential of water is not connected with a certain electric field in the bulk dielectric.

2. Breakdown occurs at a specific current density.

3. The hydrogen evolution reaction plays an important part as far as the cathode is concerned. The lower the exchange current density, the higher is the breakdown potential.

4. The glow seen at the electrodes is probably due to the plasma discharge in a steam-hydrogen gas layer formed at the water-electrode interface.

5. The breakdown potential is the potential at which the Fermi level of the cathode becomes equal to the energy of the bottom up the conduction band of liquid water. Under such conditions electrons can be readily transferred from the cathode to the anode without interaction with water molecules. At the anode, holes would enter the valency band for water.

6. The head of the so-called streamers is occupied by electrons moving in the conductivity band of water at a rate too high for chemical interaction to occur.

7. The breakdown potential can be modified by the use of adsorbed layers of materials, and the storage in water can be increased by some ten times by the use of such coatings.

REFERENCES

1. A. H. Sharbough, J. C. Devins, and S. Z. Rzad, *IEEE Trans. Electr. Insul.*, **EI-13**, 249 (1978).
2. W. G. Chadband, *J. Phys. D.*, **13**, 1299 (1980).
3. J. C. Devins, S. J. Rzad, and R. J. Schwabe, *J. Appl. Phys.*, **52**, 4531 (1981).
4. R. E. Hebner, E. F. Kelly, E. D. Forster, and G. J. Fitzpatrick, in Proceedings of 8th International Conference Conduction and Breakdown in Dielectric Liquids, IEEE 84CH2055-2, p. 185 (1984).
5. R. E. Hebner, E. F. Kelly, E. D. Forster, and G. J. Fitzpatrick, 1983 Annual Report, Conference on Electrical Insulation and Dielectric Phenomena, IEEE 83CH1902-6, pp. 26-34 (1983).
6. R. E. Hebner, E. F. Kelly, E. D. Forster, and G. J. Fitzpatrick, *J. Electrostatics*, **12**, 265 (1982).
7. P. B. McGrath and P. J. McKenny, *ibid.*, **12**, 241 (1982).
8. H. Yamashita, H. Amano, and T. Mori, *J. Phys. D.*, **10**, 1753 (1977).
9. E. O. Forster and P. Wong, Conference Record, IEEE International Symposium on Electrical Insulation, 78CH1287-2-EI, pp. 242-244 (1978).
10. R. N. Allan and E. M. Hizal, *Proc. IEEE*, **121**, 227 (1974).
11. E. O. Forster and P. P. Wong, Conference Record, IEEE International Symposium on Electrical Insulation, 80CH1496-9EI, pp. 222-224 (1980).
12. E. O. Forster, *IEEE Trans. Electric Insul.*, **EI-15**, 182 (1980).
13. T. M. Sufiar and W. G. Chadband, 1983 Annual Report, Conference on Electrical Insulation and Dielectric Phenomena, IEEE 83CH1902-6, pp. 20-25 (1983).
14. M. Zahn, T. Takada, and S. Voldman, *J. Appl. Phys.*, **54**, 4749 (1983).
15. E. O. Forster, *IEEE Trans. Electr. Insul.*, **EI-20**, 905 (1985).
16. J. Sobkowski and M. Szklarczyk, *Electrochim. Acta*, **25**, 383 (1980).
17. M. Szklarczyk, A. Czerwinski, and J. Sobkowski, *J. Electroanal. Chem.*, **132**, 263 (1982).
18. J. O'M. Bockris and A. K. N. Reddy, "Modern Electrochemistry," Rosetta ed., Plenum Press, New York (1977).
19. H. H. Skilling, "Fundamentals of Electric Waves," John Wiley & Sons, Inc., New York (1948).
20. J. O'M. Bockris, D. Drazic, and A. R. Despic, *Electrochim. Acta*, **4**, 325 (1961).
21. A. Despic and J. O'M. Bockris, *J. Chem. Phys.*, **32**, 319 (1960).
22. L. I. Krishtalik, "Charge Transfer Reactions in Electrochemical and Chemical Processes," Consultants Bureau, New York (1986).
23. J. S. Clements, M. Sato, and R. H. Davis, *IEEE Trans. Ind. Appl.*, **IA-23**, 224 (1987).
24. T. Watanabe and H. Gerischer, *J. Electroanal. Chem.*, **122**, 73 (1981).

25. J. O'M. Bockris and S. U. M. Khan, "Quantum Electrochemistry," Plenum Press, New York (1979).
26. E. J. Hart and J. W. Boag, *J. Am. Chem. Soc.*, **89**, 4090 (1962).
27. P. Delahoy and V. S. Srinivasan, *J. Phys. Chem.*, **20**, 520 (1966).
28. G. C. Barker, B. Stringer, and M. J. Williams, *J. Electro-*
anal. Chem., **51**, 305 (1974).
29. K. Johnson, Private communication.
30. M. Neuberger, "III-V Semiconducting Compounds," Plenum Press, New York (1971).
31. J. O'M. Bockris, *Nature*, **158**, 584 (1946).
32. "Handbook of Physics and Chemistry," R. C. Weast, Editor, CRC Press, Boca Raton, FL (1982).

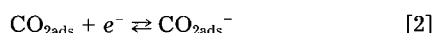# The Photoelectrocatalytic Reduction of Carbon Dioxide

J. O'M. Bockris* and J. C. Wass**

Department of Chemistry, Texas A&M University, College Station, Texas 77843

ABSTRACT

The kinetics of the photoreduction of CO_2 in nonaqueous solutions containing tetraalkyl ammonium cations has been examined with special reference to the effects of surface decoration of p-CdTe with metals, organic complexes, and crown ethers. The electrode surface was scanned by SEM, XPS, and particularly by FTIR spectroscopy. The principal product throughout was CO, although small amounts of formate and methanol were observed. Catalysts, except for the crown ethers, produce an anodic shift in the i-V curves which is in the region of 100-200 mV, equivalent to ≈ 10 times increases in the rate constant. The efficiency of the conversion of light to CO is $\approx 5\%$. Crown ethers adsorb on the surface in a lying down position and behave in a pseudo-Langmuirian way. The 18-crown-6 ether in the presence of tetraethyl ammonium cations produces the greatest catalysis, a 410 mV shift, equivalent to about 10^3 times increase in the rate constant. The photoelectrochemical kinetic parameters are consistent with a rate-determining step, $CO_2 + H^+ + e + h\nu \rightarrow CO + OH^-$. The catalyst effect of the NR_4^+ ions is interpreted in terms of the foregoing electrochemical reactions, $NR_4^+ + e \leftrightarrows NR_4$ and $NR_4 + CO_2 \rightleftarrows NR_4^+ + CO_2^-$ which take place on different sites from that of the photoelectrochemical reactions. The catalytic shifts are correlated with changes in bonding between intermediate radicals and the catalyst atoms as in electrochemical catalysis.

The electrochemical reduction of carbon dioxide has been well researched (1-3), first on metals (4-33), then at n-type semiconductors (34-41), and p-type semiconductors (42-55), and illuminated semiconducting powders (35, 56-62). The standard thermodynamic equilibrium potentials for the reduction of carbon dioxide to various products are in the range −0.2 to +0.17V (1). The mechanism of reduction has been the source of much controversy. Recently, the work of Chandrasekaran and Bockris (63), which involved detection and measurement of intermediate radicals by the use of *in situ* FTIR spectroscopy, made it likely that the sequence of the reaction is as follows (27, 28, 64, 65)

$$CO_{2aq} \rightleftarrows CO_{2ads} \qquad [1]$$

$$CO_{2ads} + e^- \rightleftarrows CO_{2ads}^- \qquad [2]$$

$$CO_{2ads}^- + H_2O + e^- \rightarrow HCOO^- + OH^- \qquad [3]$$

The photoelectrochemical reduction of CO_2 has been studied to a much less degree (38, 39). However, it has great interest because photosynthesis can be interpreted in terms of electrochemical mechanisms (66), and because of the possibility that artificial photocells could be contrived which would give rise to the economic reduction of CO_2 in the presence of light, to form products of interest, e.g., methanol.

Investigations have been made which involved the study of photocurrent-potential relations as a function of the catalyst type and content on the semiconductor electrode. In parallel, spectroscopic examinations of the structure of the adsorbed layers have been carried out.

The solutions used for these studies have involved largely nonaqueous solvents, in particular DMF. Aprotic solvents have advantages for CO_2 reduction to CO in that hydrogen evolution which competes with CO_2 reduction can be suppressed and the solubility of CO_2 is greater (67-69) than in aqueous solutions. Based upon the studies of Aurian-Blajeni *et al.* (70), however, it has been found helpful to add 1-5% of water.

Experimental

Phosphorous-doped single crystals of p-cadmium telluride (100), 1 mm thick ($N_D = 8 \times 10^{16}$ cm^{-3}), were obtained from SERI as a gift. The specific resistance was 1.5×10^3 Ω cm. Boron-doped single crystal p-silicon (100) ($N_D = 9 \times 10^{16}$ cm^{-3}) was bought from Rockwell International. The resistivity was 0.03 Ω cm. Electrode materials were sonicated in methanol for 15 min and rinsed with triply distilled water before electrode preparation.

Part of the treatment of the semiconductor electrodes in preparation for photoelectrochemical measurements involves etching the crystal (71). The p-CdTe electrodes were etched with aqua regia for 30s followed by a 5s washing with triply distilled water and a drying under a stream of argon. The p-Si electrodes were etched with the hydrofluoric acid aqua regia mixture (1:1) for 5 min followed by a 5s washing in triply distilled water and dried under a stream of argon. This procedure was carried out three times successively.

In accordance with the catalytic effects noted by Taniguchi *et al.* (72), and supported by other work (73), arising from the use of ammonium salts as supporting electrolytes, tetraalkyl ammonium salts (Fluka) were used as such after recrystallization from ethanol. The solvent for the photoelectrochemical investigations, N,N-dimethylformamide (Fischer Scientific) was used without further purification. Gas chromatographic analysis was used to verify that less than 0.5% degradation products were present before use. $LiClO_4$ and LiF dissolved in HPLC grade acetonitrile (Fischer Scientific) were the solvents used for spectroscopic investigations. Triply distilled and pyrolyzed water were used to prepare aqueous solutions.

The experiments were carried out under potentiostatic conditions using a Stonehart Associates, Incorporated, potentiostat, Model BC1200 and a PAR programmer, Model 175. Irradiation was performed with an Oriel Corporation lamp, Model 6136 and a Bausch & Lomb high-intensity monochromator no. 33-86-76. All photoassisted controlled potential electrolysis (CPE) experiments were carried out at room temperature, 560 nm illumination wavelength (0.5 mW cm^{-2}), under a blanket of argon or carbon dioxide after purification (43-45, 74).